Materials and Design 45 (2013) 532–538

Contents lists available at SciVerse ScienceDirect

Materials and Design

journal homepage: www.elsevier.com/locate/matdes

Effects of volume fraction on the microstructure and tensile properties of *in situ* TiBw/Ti6Al4V composites with novel network microstructure

L.J. Huang [a,b], L. Geng [a,*], B. Wang [a], L.Z. Wu [b]

[a] School of Materials Science and Engineering, Harbin Institute of Technology, P.O. Box 433, Harbin 150001, China
[b] Center for Composite Materials and Structures, Harbin Institute of Technology, P.O. Box 3010, Harbin 150080, China

ARTICLE INFO

Article history:
Received 3 September 2012
Accepted 25 September 2012
Available online 4 October 2012

Keywords:
Titanium matrix composites
Microstructures
Mechanical properties
Volume fraction
Powder metallurgy

ABSTRACT

In order to better understand the relationship of structure–mechanical properties of TiBw/Ti6Al4V (TiBw/Ti64) composites with a network microstructure and deduce the upper limit of TiBw volume fraction, the effects of volume fraction on the microstructure and tensile properties were further investigated. The equation calculating the optimal and maximum volume fractions of reinforcement for the composites with a network microstructure was deduced. For the present system, the optimal and maximum volume fractions were verified to be 5.1 vol.% and 10.2 vol.%, respectively, by calculation, microstructure observation, tensile properties. When the volume fraction was equal and lower than 5.1 vol.%, the coarse TiBw formed, or else, the fine TiBw, the cluster TiBw and the block TiBw, even unhealed pores formed. The tensile strength of TiBw/Ti64 composites increases and then hastily decreases, while the ductility keeps on decreasing with increasing volume fractions of TiBw reinforcement.

1. Introduction

Due to their high special strength, high special stiffness, excellent wear resistance and high temperature durability, titanium matrix composites (TMCs) attract more and more attention which render them as the optimal candidate material for a range of commercial automotive, aerospace and military applications [1–3]. Due to their superior and isotropic properties and low cost, the discontinuously reinforced titanium matrix composites (DRTMCs) fabricated by *in situ* methods are quite sought-after [4–8]. Moreover, the *in situ* synthesized TiB whisker (TiBw) reinforcement is recognized to be the most compatible and effective reinforcement for Ti matrix [1,3]. According to published work [1,3,6,9], the majority of DRTMCs including TiBw/Ti composites with a homogeneous microstructure has been prepared by the conventional powder metallurgy (PM) process including high-energy milling, isostatic cool pressing and sintering, because the PM process has exhibited the ability for microstructural control, near net shape processing, minimal material waste and low cost [3,9]. However, DRTMCs fabricated by the conventional PM process face a severe challenge of low fracture ductility, even extreme brittleness [1,3,6,9], which seriously restricts their practical applications.

A novel network microstructure of TiBw/Ti64 composites has been successfully designed and fabricated by tailoring the distribution of TiBw reinforcement [10,11]. Both the strengthening effect of TiBw reinforcement and the toughening effect of Ti64 matrix of the TiBw/Ti64 composites with a network microstructure are much better utilized than the composites with a homogenous microstructure. It is worth noting that the novel network microstructure can be viewed as the Hashin–Shtrikman (H–S) upper bound structure [12,13] or the multi-scale hierarchical structures proposed by Lu [14]: compared with conventional or homogeneous composite structure, the strengthening ratio can be further enhanced by assembling components in a controlled way to form a novel reinforcements or hierarchical structure [14]. The superior performances of the novel composites have been sufficiently exhibited in the previous work [10,11,15]. Moreover, the fabrication process of the novel composite is consistent with proposal by Morsi and Patel [3]: using low-energy processing approaches and the microstructural design, respectively.

However, for this novel composite, the mechanical property is highly sensitive to the reinforcement volume fraction on the boundary. Additionally, designing the volume fraction is important to get one superior mechanical property. Therefore, it is necessary to construct one method to design the reinforcement volume fraction and predict the mechanical property. In the present study, the aim is to deduce one equation which can predict the optimal and the maximum reinforcement volume fractions of the novel composite, by design, microstructure observation and performance analysis. It is also the first time to get one useful equation to predict the upper limit of the reinforcement volume fraction of DRTMCs to date [9]. This equation is useful and also important to

* Corresponding author. Tel.: +86 451 86418836; fax: +86 451 86413922.
E-mail addresses: ljhuanghit@yahoo.com.cn, huanglujun@hit.edu.cn (L.J. Huang).

0261-3069/$ - see front matter Crown Copyright © 2012 Published by Elsevier Ltd. All rights reserved.
http://dx.doi.org/10.1016/j.matdes.2012.09.043

design microstructure and mechanical properties in the area of metal matrix composites fabricated by powder metallurgy routes. Furthermore, the effects of reinforcement volume fraction on the microstructure and tensile properties are useful and important to understand the relationship of structure–mechanical properties of the novel composites.

2. Experimental procedures

In order to better understand the relationship of structure and mechanical properties of TiBw/Ti64 composites with a network microstructure, a range of TiBw/Ti64 composites with different volume fractions have been fabricated using identical processes and raw materials. Fig. 1 shows the flow chart and SEM micrographs of raw materials and mixture. The large and spherical Ti64 powders with an average size of 200 μm (Fig. 1a), prismatic TiB_2 powders with an average size of 3 μm (Fig. 1b) were employed in the present study in order to construct the novel network microstructure. The two raw materials were milled at the speed of 200 rpm and with a ratio of milling media to material of 5:1 for 8 h using a planetary blender under an argon atmosphere, instead of high-energy milling process of conventional PM route. The aim of low-energy milling process is not to break down the large Ti64 powders but to adhere fine TiB_2 powders onto the surface of the large Ti64 powders as shown in Fig. 1c and d. The mixture (Fig. 1c) was directly transferred into graphite mould and then sintered in a vacuum atmosphere (10^{-2} Pa) with a heating rate of 10 °C/min, and then hot pressed at 1200 °C under a pressure of 20 MPa for 1 h. The TiB whiskers were *in situ* synthesized according to the following reaction equation:

$$\begin{array}{lccccc} & \mathrm{Ti} & + & \mathrm{TiB_2} & \rightarrow & 2\mathrm{TiB} \\ \text{Molar mass :} & 47.9 & & 69.52 & & 117.42 \\ \text{Actual mass :} & \frac{47.9\ \mathrm{wt.\%TiB_2}}{69.52}\cdot \mathrm{X} & & \mathrm{wt.\%TiB_2}\cdot \mathrm{X} & & \frac{117.42\ \mathrm{wt.\%TiB_2}}{69.52}\cdot \mathrm{X} \end{array} \quad (1)$$

On the basis of the Eq. (1), the correlation between the wt.% TiB_2 added and the vol.% TiBw synthesized can be expressed as the following equations:

$$\mathrm{Vol.\%TiB} = \frac{V_{\mathrm{TiB}}}{V_{\mathrm{TiB}} + V_{\mathrm{remained-Ti}}} \times 100\% \quad (2)$$

$$= \frac{\frac{117.42\ \mathrm{wt.\%TiB_2}}{69.52\rho_{\mathrm{TiB}}}\cdot \mathrm{X}}{\frac{117.42\ \mathrm{wt.\%TiB_2}}{69.52\rho_{\mathrm{TiB}}}\cdot \mathrm{X} + \frac{(1-\mathrm{wt.\%TiB_2})\cdot \mathrm{X} - \frac{47.9\ \mathrm{wt.\%TiB_2}}{69.52}\mathrm{X}}{\rho_{\mathrm{Ti}}}} \quad (3)$$

where X is the total mass of the mixed material. Taking the ρ_{TiB} and ρ_{Ti} values of 4.5 and 4.45 g/cm^3 for TiB density and Ti64 density into Eq. (3), the equation between wt.% TiB_2 and vol.% TiBw can be simplified to the following equation:

$$\mathrm{vol.\%TiB} = 1.7 \times \mathrm{wt.\%TiB_2} \quad (4)$$

According to the Eqs. (1) and (4), 1.7 vol.%, 3.4 vol.%, 5.1 vol.%, 6.8 vol.%, 8.5 vol.% and 10.2 vol.% TiBw/Ti64 composites were designed and fabricated by adding 1 wt.%, 2 wt.%, 3 wt.%, 4 wt.%, 5 wt.%, 6 wt.% TiB_2 raw materials.

Room temperature tensile tests, which refers to the metal materials testing standards of ISO 6892: 1998 [16], were carried out using an Instron-5569 universal testing machine at a constant crosshead speed of 0.5 mm/min (approximate strain rate is 5.5×10^{-4}/s). A total of five tensile samples with dimensions of 15 mm × 5 mm × 2 mm were tested for each material. Microstructural and fracture characterizations were examined using a scanning electron microscope (SEM, Hitachi S-4700). The samples for microstructure observation were etched using the Kroll's solution (5 vol% HF + 10 vol.% HNO_3 + 85 vol.% H_2O) for 10 s after mechanical polishing.

3. Results and discussions

3.1. Design of the reinforcement volume fraction

In order to design the optimal and the maximum volume fractions of reinforcement for TiBw/Ti64 composites with a network microstructure, two schematic illustrations of Ti64 and TiB_2 mixture were constructed as shown in Fig. 2. Fig. 2a shows that half surface of every Ti64 particle is covered by fine TiB_2 powders. For this case, all TiB_2 powders have the same opportunity to contact with Ti64 particle when the loose mixtures are sintered to compact mixtures of Ti64 and TiB_2. Then, the reaction between Ti and TiB_2 can be rapidly completed, which causes the synthesis of coarse TiBw reinforcement [10]. In order to simplify the calculation process, the TiB_2 powders were also assumed to be spherical due to their large size difference between Ti64 and TiB_2 powders. For this case, the weight ratio of TiB_2 powder to Ti64 particle can be expressed as follows:

$$\frac{m}{M} = \frac{\frac{4}{3}\pi r^3 \cdot \rho_1 \cdot \frac{1}{2} \times \frac{4\pi(R+r)^2}{\pi r^2}}{\frac{4}{3}\pi R^3 \cdot \rho_2} \quad (5)$$

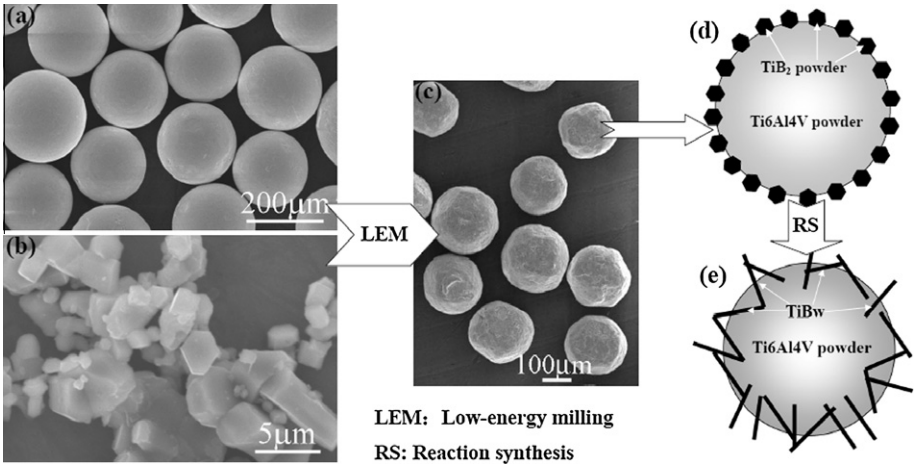

Fig. 1. Flow chart showing the processing route together with SEM micrographs of raw materials and schematic illustrations of network distribution. (a) Ti64 powders (200 μm), (b) TiB_2 powders (3 μm), (c) the blended mixture, and schematic illustrations of network distribution (d) before and (e) after reaction synthesis.

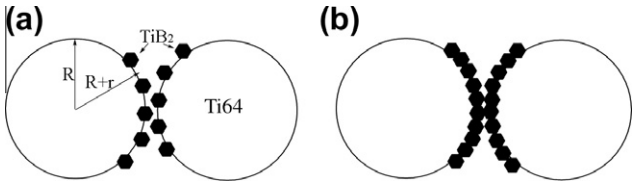

Fig. 2. Schematic illustrations of fine TiB_2 powders onto the surface of large Ti64 particles. (a) a half surface of Ti64 is covered by TiB_2, (b) the whole surface of Ti64 is covered by TiB_2.

$$= \frac{2(R+r)^2 \cdot r \cdot \rho_1}{R^3 \cdot \rho_2} \tag{6}$$

where m, r and ρ_1 are the weight, radius and density of TiB_2 powders, respectively, and M, R and ρ_2 are those of Ti64 particles.

And then the calculation equation for the volume fraction (V_{TiB}) of *in situ* synthesized TiBw can be deduced by taking Eq. (6) into Eq. (4), which can be expressed as follows:

$$V_{TiB} = \frac{3.4(R+r)^2 \cdot r \cdot \rho_1}{R^3 \cdot \rho_2 + 2(R+r)^2 \cdot r \cdot \rho_1} \tag{7}$$

Taking the R and ρ_2 values of 100 μm and 4.45 g/cm^3 for Ti64 particles and r and ρ_1 values of 1.5 μm and 4.52 g/cm^3 for TiB_2 powders into Eqs. (6) and (7), the wt.% TiB_2 and vol.% TiBw for the present case can be calculated to be approximately 3 wt.% and 5.1 vol.%, respectively.

Accordingly, when the whole surface of the Ti64 particle is covered by TiB_2 powders as shown in Fig. 2b, the wt.% TiB_2 and vol.% TiBw are 6 wt.% and 10.2 vol.%. For this case, the outside of TiB_2 powder cannot easily touch with Ti and transformed to TiB whisker. Therefore, the reaction between Ti and TiB_2 cannot be rapidly completed to synthesize coarse TiBw reinforcement. One similar phenomenal that fine TiBw and cluster TiBw formed when Ti is insufficient [17].

According to the calculation results, when the designed volume fraction of TiBw reinforcement is lower than the equal of 5.1 vol.%, just coarse and strong TiB whiskers are *in situ* synthesized. The strengthening effect increases with increasing volume fraction of TiBw reinforcement. Once the volume fraction exceeds 5.1 vol.%, fine TiBw and even cluster TiBw formed, and the quantities of them increase with increasing the designed volume fraction according to the calculation results. In order to further demonstrate the calculation results and investigate the microstructure evolution, 1.7 vol.%, 3.4 vol.%, 5.1 vol.%, 6.8 vol.%, 8.5 vol.% and 10.2 vol.% TiBw/Ti64 composites were fabricated and analyzed as follows.

3.2. Microstructure

As shown in Fig. 1e, TiB whiskers are *in situ* synthesized at the local places around the boundary of Ti64 particle, and then formed into a network structure as shown in Fig. 3. Fig. 3 shows SEM micrographs of 3.4 vol.% and 10.2 vol.% TiBw/Ti64 composites with a network microstructure. (1) The network structure is formed in both composites due to the use of large Ti64 particles and low energy milling process. (2) The network structure can be divided into one TiBw-lean region (TLR) and one TiBw-rich boundary region (TRBR). (3) The TiBw/Ti64 composite with a lower volume fraction can be easily compacted, but unhealed pores are remained in the composite with a maximum volume fraction (Fig. 3b). On the one hand, the deformation resistance is too high to compact the composite with a much higher volume fraction of reinforcement. On the other hand, because the whole surface of every Ti64 particle is covered by TiB_2 ceramic phase, the sintering system is close to ceramic system as shown in Fig. 2b. The densification of ceramic system needs higher conditions than those for metal or general composite systems.

Fig. 4 shows SEM micrographs of 1.7 vol.%–10.2 vol% TiBw/Ti64 composites with a network microstructure in order to reveal the microstructure evolution of *in situ* synthesized reinforcement. The local volume fraction of the TiBw in the network boundary increases with increasing overall volume fractions of TiBw. That is to say, the contiguity of TiBw increases with increasing volume fractions. The network boundary/TRBR becomes continuous; in other words, the matrix particle/TLR does discrete, when the reinforcement volume fraction is over 10.2 vol% as shown in Figs. 3b and 4f. That is to say, one 3D compact ceramic shell formed during sintering process encapsulates the discrete Ti64 matrix particle. When the volume fraction is lower than 10.2 vol.%, the TLR is interpenetrated through TRBR (Fig. 4a–e). It is certain that the contiguity of matrix correspondingly decreases with increasing volume fraction of TiBw reinforcement. When the volume fraction is lower than 5.1 vol.%, TiB_2 powders are completely transformed to the coarse and strong TiBw reinforcement, which can link the adjacent matrix particles as dowel connectors as shown in Fig. 4a–c. This is consistent with the design as shown Fig. 2a. When the designed volume fraction is up to 6.8 vol.%, fine TiBw and cluster TiBw are observed (Fig. 4d). In the previous literatures, Ni et al. [17] and Patel et al. [18] have pointed out that the formation of cluster TiBw is due to the large B_4C raw material and high volume fraction at the local region. In summary, the formation of cluster TiBw can be attributed to the excessive TiB_2 or insufficient Ti at the local region. When the designed volume fraction is continuously increased to 8.5 vol.% and 10.2 vol.%, even block TiBw is formed due to the much high local volume fraction (Fig. 4e and f). That is to say, the designed 6.8 vol.% has already exceeded the optimal volume fraction for the present system. It is certain that the coarse TiBw is beneficial while the cluster and the block TiBw are harmful to the tensile ductility of the present composites with a network microstructure. Therefore, 5.1 vol.% and 10.2 vol.% may be the optimal and maximum reinforcement volume fraction for the present system (Fig. 2).

Fig. 5 shows SEM micrographs of 1.7 vol.% and 10.2 vol.% TiBw/Ti64 composites at a higher magnification. Together with Fig. 4 and our previous work [10,16], it can be concluded that not only one single TiB whisker but also branched whiskers are formed in the composites with a network microstructure, and the quantity of branched whiskers increases with increasing the wt.% TiB_2 addition. However, it can be also concluded that the claw-like whiskers as shown in the Fig. 5a are formed due to the polycrystal TiB_2 raw material considering the much low wt.% TiB_2 addition and the previous work [16]. As shown in Fig. 5b, it is observed that the block reinforcement boundary is made of fine TiBw and TiBw agglomerations besides coarse TiBw. The formation of fine whiskers and agglomeration is due to the excessive TiB_2 at the local region, which can be verified by the similar observation (micron TiBw and TiBw clusters) reported by Patel et al. [18]. Another evidence is that the coarse TiB whiskers just can be synthesized by the inside part of TiB_2 powder embedded around the surface of Ti64 particle.

3.3. Tensile properties

Fig. 6a shows the tensile strain–stress curves of TiBw/Ti64 composites with different volume fractions of reinforcement. The variations of the ultimate tensile strength (σ_b) and elongation (δ) with increasing the volume fractions are shown in Fig. 6b. It can be clearly seen that σ_b increases with increasing volume fractions from 0 vol.% to 6.8 vol.% and then decreases from 6.8 vol.% to 10.2 vol.%. The former increase of σ_b can be attributed to the increasing local volume fraction in the TRBR, while the latter decrease of σ_b to the formation of cluster TiBw, block TiBw and un-

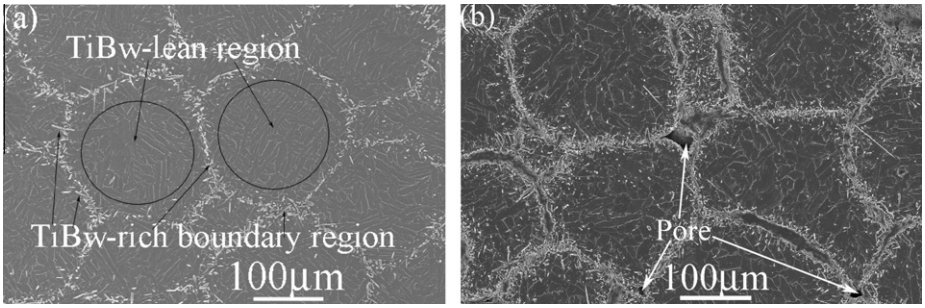

Fig. 3. SEM micrographs of (a) 3.4 vol.% and (b) 10.2 vol.% TiBw/Ti64 composites with a network microstructure at a low magnification.

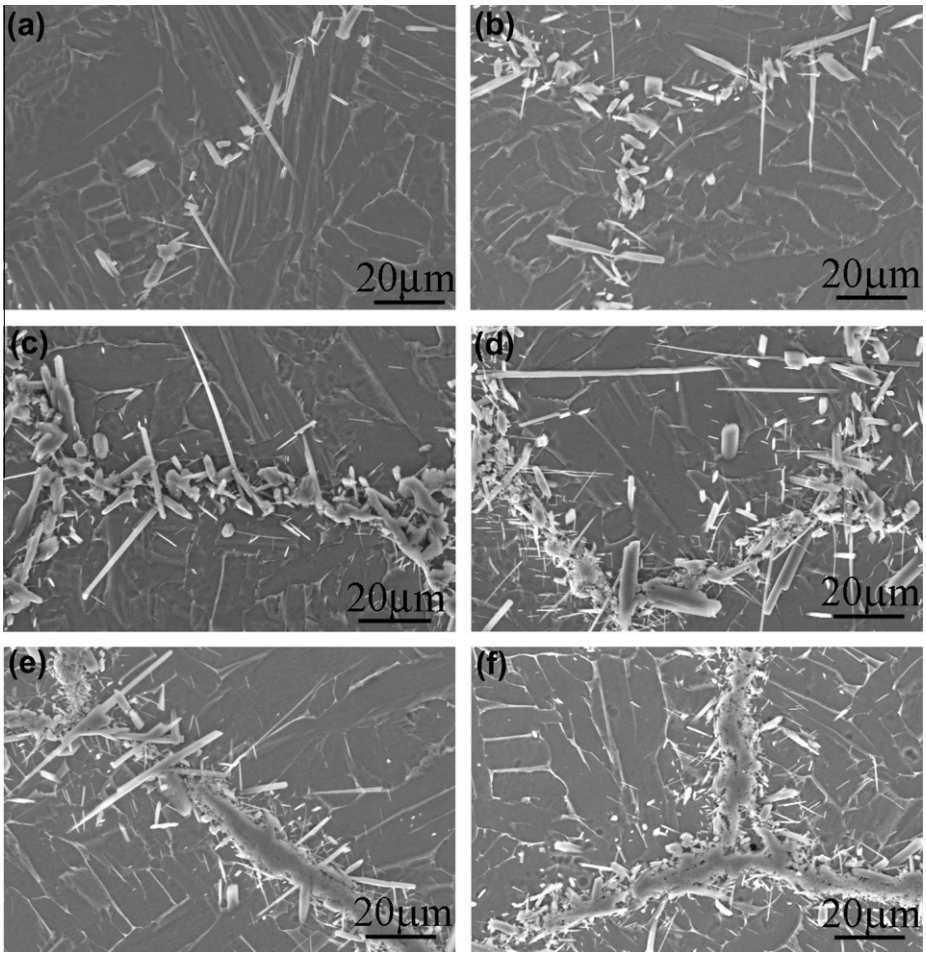

Fig. 4. SEM micrographs of TiBw/Ti64 composites with different volume fractions and the same network distribution of TiBw reinforcement. (a) 1.7 vol.%, (b) 3.4 vol.%, (c) 5.1 vol.%, (d) 6.8 vol.%, (e) 8.5 vol.%, (f) 10.2 vol.%.

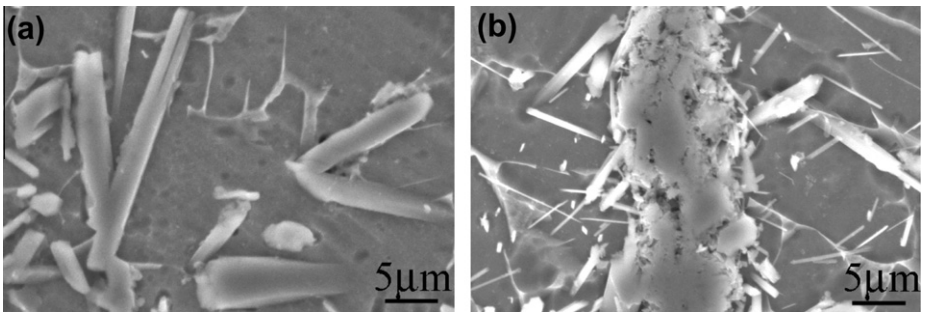

Fig. 5. SEM micrographs of 1.7 vol.% (a) and 10.2 vol.% (b) TiBw/Ti64 composites at a high magnification.

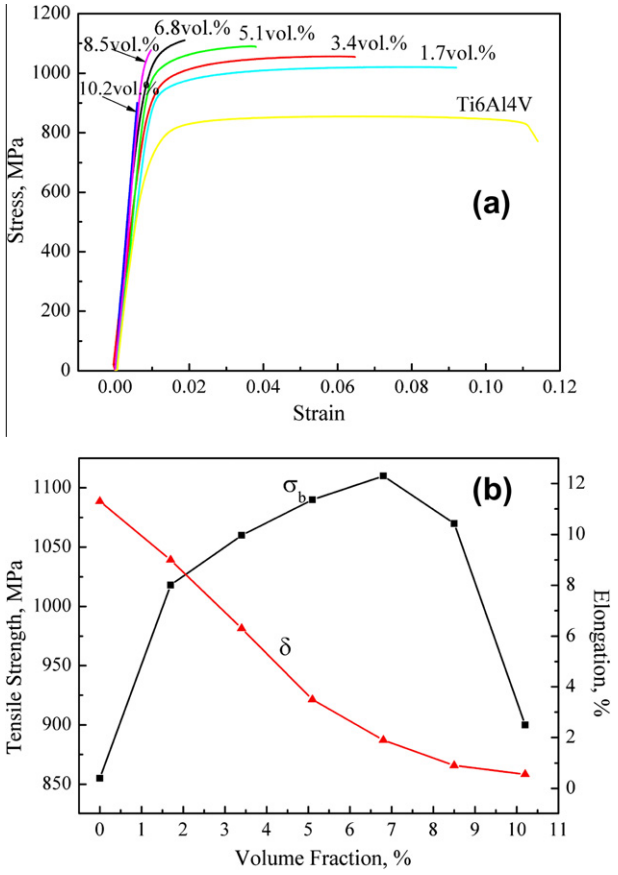

Fig. 6. Tensile strain–stress curves (a) and the variation of tensile properties (b) of TiBw/Ti64 composites with different volume fractions of TiBw reinforcement.

healed pores as shown in Fig. 4d–f. The strength is increased to 1021 MPa (or by 19.4%) just by the *in situ* synthesis of 1.7 vol.% TiBw reinforcement. Even, the highest σ_b is increased to 1110 MPa from 855 MPa, which is equivalent to an increment of 30%. These phenomena demonstrate the effective strengthening effect of the reinforcement network structure, which can be attributed to the dowel-like TiBw connectors, branched TiBw and the novel network structure [11]. Compared with the composites fabricated by casting technique + PM process + hot deformation [19,20], the present strengthening effect can be also viewed as a superior strengthening effect.

The strength is sharply decreased to 897 MPa when the volume fraction is up to the maximum 10.2 vol.%. The tensile elongation keeps on decreasing with increasing the volume fraction, which can be attributed to the decreasing contiguity of TLR. It is worth noting that the tensile elongations of the 1.7 vol.%, 3.4 vol.% and 5.1 vol.% TiBw/Ti64 composites can reach to 9.0%, 6.3% and 3.5%, which are significantly improved by tailoring the network reinforcement distribution compared with those of conventional composites with a homogeneous reinforcement distribution [1,3,6]. It is worth pointing out that the present composites are successfully fabricated just by one simplified process including low-energy milling and sintering without any subsequent treatment such as extrusion. The good ductility can be attributed to the interpenetrating matrix phase through TRBR and the large size of TLR.

3.4. Strengthening and toughening behaviors

The size of plastic zone at the tip of crack can be expressed as following [21]:

$$D = \frac{1}{2\pi}\left(\frac{K_I}{\sigma_{ys}}\right)^2 \tag{8}$$

The schematic illustrations of the different plastic zones of the composites with a network structure are shown in Fig. 7. For the composites with a lower volume fraction in TRBR, σ_{ys} is relatively low and K_I is relatively higher. Therefore, a much larger plastic zone D exists around TRBR of the composite with a much lower volume fraction of reinforcement, which can effectively restrict the crack propagation, decrease the crack propagation rate and then encourage TLR to bear plastic strain [11]. Therefore, the strengthening effect of TiBw reinforcement and the toughening effect of the Ti64 matrix can be better utilized through this novel network structure. However, with increasing volume fractions of TiBw, not only σ_{ys} increases but also K_I decreases for the composites with a network microstructure, which lead to a remarkably decrease of the plastic zone size D at the tip of crack in the network boundary (Fig. 7b). Therefore, less and less TLR bears strain, and the crack propagation rate increases. Additionally, more and more TiBw without bearing stress are cracked by crack tip stress, even unstable crack propagation (10.2 vol.%), due to too high volume fraction. That is to say, the strengthening effect of TiBw reinforcement and toughening effect of Ti64 matrix are less utilized for the composites with too high volume fraction, which leads to that both tensile strength and elongation decreases with increasing volume fractions after the optimal reinforcement volume fraction (Fig. 6b).

3.5. Fracture behavior

Fig. 8 shows SEM fractographs of 1.7 vol.%, 10.2 vol.% TiBw/Ti64 composites with a network microstructure under tensile testing. Together with the fracture surface of 5.1 vol.% TiBw/Ti64 composite [11], it can be concluded that the fracture mechanism changes with increasing the volume fraction. It can be seen from Fig. 8a that

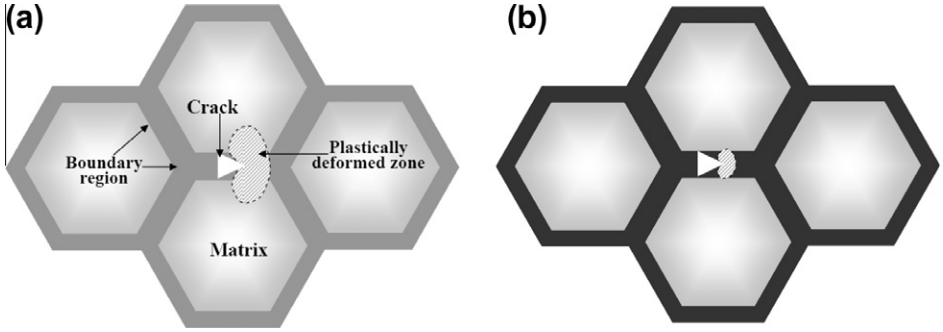

Fig. 7. Schematic illustrations of the influence of local reinforcement volume fraction on the plastic zone size during fracture for the composites with a lower (a) and higher (b) reinforcement volume fraction.

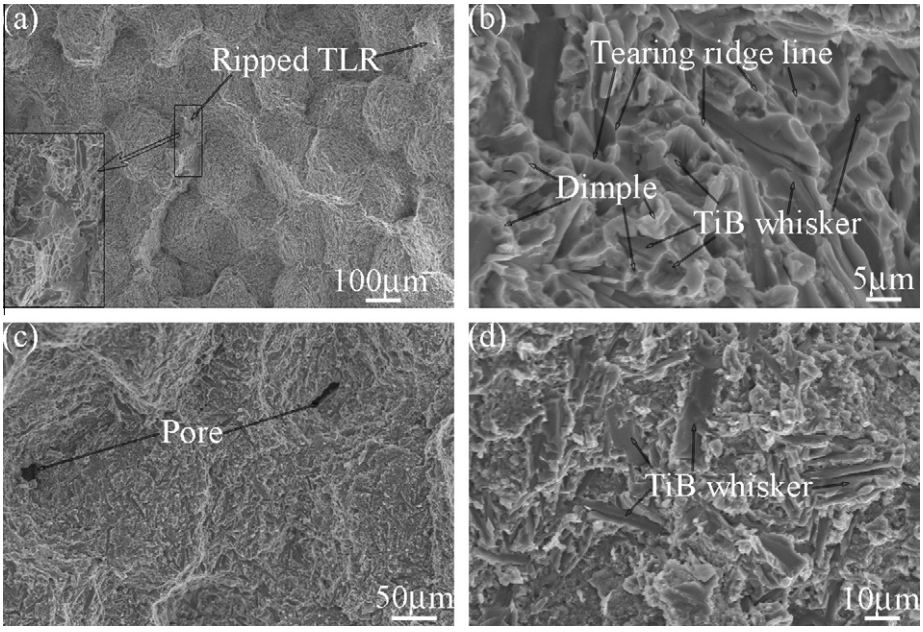

Fig. 8. SEM fractographs of 1.7 vol.% and 10.2 vol.% TiBw/Ti64 composites. (a and b) 1.7 vol.% TiBw/Ti64 composite, (c and d) 10.2 vol.% TiBw/Ti64 composite; (a and c) at lower magnifications, (b and d) at higher magnifications.

some TLRs are ripped besides the main cleavage fracture of TRBRs. Partly plastic deformation of TLR prior to failure indicates a superior ductility, and the local dimples and tearing ridge lines around broken whisker at boundary region (Fig. 8b) indicates that the interpenetrating TLR can also play an obvious toughening effect. The ripped TLRs, dimples and tearing ridge lines at TRBR are quite consistent with a tensile elongation of 9%. Additionally, the majority broken whiskers as shown in Fig. 8b indicates a superior strengthening effect, which corresponds to a steep increase (19.4%) of the ultimate strength (Fig. 6a and b). Further increasing the volume fraction of reinforcement absolutely decreases the fraction of dimples and tearing ridge lines, which corresponds to the shrinking plastic zone at the tip of crack in TRBR and decreases the ductility of the composites (Figs. 6 and 7).

However, not only the ripped TLRs disappear but also dimples and tearing ridge lines in TRBR disappear, which remarkably decrease the ductility or increase the brittleness of 10.2 vol.% TiBw/Ti64 composite as shown in Fig. 8c and d. Moreover, the unhealed pores acting as the origins of crack worsen the tensile properties (Fig. 8c). Not dimples and tearing ridge lines but a typical ceramic brittle fracture around broken whiskers is quite consistent with the block reinforcement boundary (Figs. 4f and 5b) and inferior tensile properties (Fig. 6).

In summary, 5.1 vol.% can be regarded as the optimal volume fraction while 10.2 vol.% as the maximum volume fraction for the present system of spherical Ti64 powders with a diameter of 200 μm and TiB_2 powders with that of 3 μm. It is worth pointing out that the optimal and maximum volume fractions can be further increased by decreasing the Ti64 particle size or increasing the TiB_2 powder size according to Eq. (7).

4. Conclusions

(1) The tensile strength of TiBw/Ti64 composites increases and then hastily decreases, while the ductility keeps on decreasing with increasing volume fractions of TiBw reinforcement.
(2) The optimal reinforcement volume fraction equation related to the size and density of matrix and reinforcement powders was deduced, which can be used to design the optimal and maximum reinforcement volume fraction of the composites with a network microstructure fabricated by powder metallurgy.
(3) The formation of the coarse TiBw can be attributed to the excessive Ti while the formation of the cluster TiBw and the block TiBw to the excessive TiB_2 at the local boundary region.
(4) With increasing volume fractions of TiBw in network boundary, the plastic zone size decreases and the crack propagation rate increases, which lead to the decrease of ductility.

Acknowledgements

This work is financially supported by the National Natural Science Foundations of China (NSFC) under Grant Nos. 51101042 and 51271064, the Fundamental Research Funds for the Central Universities under Grant No. HIT. NSRIF. 201131, the 5th-class Special Foundation (2012T50327) and the 50th-class General Foundation (2011M500653) from the China Postdoctoral Science Foundation, and the Province Heilongjiang Postdoctoral Science Foundation.

References

[1] Tjong SC, Mai YW. Processing-structure-property aspects of particulate-and whisker-reinforced titanium matrix composites. Compos Sci Technol 2008;68(3–4):583–601.
[2] Zhang C, Kong F, Xiao S, Niu H, Xu L, Chen Y. Evolution of microstructural characteristic and tensile properties during preparation of TiB/Ti composite sheet. Mater Des 2012;36:505–10.
[3] Morsi K, Patel VV. Processing and properties of titanium-titanium boride (TiBw) matrix composites – a review. J Mater Sci 2007;42(6):2037–47.
[4] Sen I, Tamirisakandala S, Miracle DB, Ramamurty U. Microstructural effects on the mechanical behavior of B-modified Ti-6Al-4V alloys. Acta Mater 2007;55(15):4983–93.
[5] Feng HB, Zhou Y, Jia DC, Meng QC. Microstructure and mechanical properties of in situ TiB reinforced Titanium matrix composites based on Ti–FeMo–B prepared by spark plasma sintering. Compos Sci Technol 2004;64(16):2495–500.
[6] Zhang ZG, Qin JN, Lu WJ, Zhang D, et al. Effect of β heat treatment temperature on microstructure and mechanical properties of in situ titanium matrix composites. Mater Des 2010;31:4269–73.

[7] Liu D, Zhang SQ, Li A, Wang HM. Creep rupture behaviors of a laser melting deposited TiC/TA15 in situ titanium matrix composite. Mater Des 2010;31:3127–33.
[8] Panda KB, Ravi Chandran KS. First principles determination of elastic constants and chemical bonding of titanium boride (TiB) on the basis of density functional theory. Acta Mater 2006;54(6):1641–57.
[9] Gorsse S, Miracle DB. Mechanical properties of Ti-6Al-4V/TiB composites with randomly oriented and aligned TiB reinforcements. Acta Mater 2003;51(9):2427–42.
[10] Huang LJ, Geng L, Peng HX, Balasubramaniam K, Wang GS. Effects of sintering parameters on the microstructure and tensile properties of *in situ* TiBw/Ti6Al4V composites with a Novel Network Architecture. Mater Des 2011;32(6):3347–53.
[11] Huang LJ, Geng L, Peng HX, Zhang J. Room temperature tensile fracture characteristics of in situ TiBw/Ti6Al4V composites with a quasi-continuous network architecture. Scripta Mater 2011;64(9):844–7.
[12] Hashin Z, Shtrikman S. A variational approach to the theory of the elastic behaviour of multiphase materials. J Mech Phys Solids 1963;11(2):127–40.
[13] Peng HX. A review of "consolidation effects on tensile properties of an elemental Al matrix composite". Mat Sci Eng A 2005;396(1–2):1–2.
[14] Lu K. The future of metals. Science 2010;328:319–20.
[15] Huang LJ, Xu HY, Wang B, Zhang YZ, Geng L. Effects of heat treatment parameters on the microstructure and mechanical properties of in situ TiBw/Ti6Al4V composite with a network architecture. Mater Des 2012;36:694–8.
[16] ISO 6892. Metallic materials-tensile testing at ambient temperature; 1998.
[17] Ni DR, Geng L, Zhang J, Zheng ZZ. Effect of B4C particle size on microstructure of in situ Titanium matrix composites prepared by reactive hot processing of Ti-B4C system. Scripta Mater 2006;55(5):429–32.
[18] Patel VV, El-Desouky A, Garay JE, Morsi K. Pressure-less and current-activated pressure-assisted sintering of titanium dual matrix composites: effect of reinforcement particle size. Mater Sci Eng A 2009;507(1–2):161–6.
[19] Boehlert CJ, Cowen CJ, Tamirisakandala S, McEldowney DJ, Miracle DB. In situ scanning electron microscopy observations of tensile deformation in a boron-modified Ti-6Al-4V alloy. Scripta Mater 2006;55:465–8.
[20] Boehlert CJ. The creep behavior of powder-metallurgy processed Ti-6Al-4V-1B(wt.%). Mat Sci Eng A 2009;510–511:434–9.
[21] Ewalds HL and Wanhill RJH. Fracture mechanics. Edward Arnold 1983.